DR LI HUANG (Orcid ID : 0000-0002-4874-0898)

Article type : - Regular Manuscript

A new mode of NPR1 action via an NB-ARC-NPR1 fusion protein negatively regulates defense response to stem rust pathogen in wheat

Xiaojing Wang[2✉*], Hongtao Zhang[2*], Bernard Nyamesorto[2*], Yi Luo[1], Xiaoqian Mu[1], Fangyan Wang[1], Zhensheng Kang[1,3], Evans Lagudah[4✉] and Li Huang[2✉]

[1] State Key Laboratory of Crop Stress Biology for Arid Areas, College of Life Sciences, Northwest A&F University, Yangling 712100, Shaanxi, China

[2]Montana State University, Department of Plant Sciences and Plant Pathology, Bozeman, MT 59717-3150, USA

[3] State Key Laboratory of Crop Stress Biology for Arid Areas, College of Plant Protection, Northwest A&F University, Yangling 712100, Shaanxi, China

[4] CSIRO Agriculture & Food, GPO Box 1700, Canberra, ACT 2601, Australia

*These authors contribute equally to the work

✉ Corresponding authors: Li Huang

Email: li.huang@montana.edu

Telephone: 1-406-994-5058

Fax: 1-406-994-7600

Evans Lagudah

Email: evans.lagudah@csiro.au

This article has been accepted for publication and undergone full peer review but has not been through the copyediting, typesetting, pagination and proofreading process, which may lead to differences between this version and the Version of Record. Please cite this article as doi: 10.1111/NPH.16748

Telephone: +61 2 6246 5392

Xiaojing Wang

Email：wangxiaojing@nwsuaf.edu.cn

Telephone：+86 02987092262

Received: *27 March 2020*

Accepted: *1 June 2020*

ORCID IDs and social media accounts of authors:

HZ: https://orcid.org/0000-0001-8231-4123,

BN: https://orcid.org/0000-0001-9723-3641,

JK: https://orcid.org/0000-0002-5863-6218,

EL: https://orcid.org/0000-0002-6234-1789,

LH: https://orcid.org/0000-0002-4874-0898,

Summary

·NPR1 has been found to be a key transcriptional regulator in some plant defense responses. There are nine *NPR1* homologs (*TaNPR1*) in wheat, but little research has been done to understand the function of those *NPR1*-like genes in wheat defense response against stem rust (*Puccinia graminius* f. sp *tritici*) pathogens.

· We used bioinformatics and reverse genetics approaches to study the expression and function of each TaNPR1.

. We found six members of TaNPR1 located on homeologous group 3 chromosomes (designated as *TaG3NPR1*) and three on homeologous group 7 chromosomes (designated as *TaG7NPR1*). The group 3 NPR1 proteins regulate transcription of SA-responsive *PR* genes. Down-regulation of all the *TaNPR1* homologs via virus induced gene co-silencing resulted in enhanced resistance to stem rust. More specifically down-regulating *TaG7NPR1* homeologs or *Ta7ANPR1* expression resulted

in stem rust resistance phenotype. In contrast, knocking down *TaG3NPR1* alone did not show visible phenotypic changes in response to the rust pathogen. Knocking out *Ta7ANPR1* enhanced resistance to stem rust. The *Ta7ANPR1* locus alternatively spliced under pathogen inoculated conditions.

· We discovered a new mode of NPR1 action in wheat at the *Ta7ANPR1* locus through an NB-ARC-NPR1 fusion protein negatively regulating defense response to stem rust infection.

Key words: NPR1; *Triticum aestivum*; Rust; Mutant; Mapping; RT-qPCR, virus-induced gene silencing (VIGS)

Introduction

Plants constantly battle with a variety of pathogens in the environment via their complex and effective innate immune systems (Spoel & Dong, 2012). Hypersensitive response (HR) is one of the strategies used to defend against biotrophic pathogens by which rapid programmed cell death occurs immediately surrounding the infection sites (Morel & Dangl, 1997) to restrict the pathogens from further spreading and replication. HR also activates a series of signals which are transduced to remote regions of the plants and generate systemic acquired resistance (SAR) with a broad-spectrum resistance to subsequent pathogen attacks (Pajerowska-Mukhtar *et al.*, 2013).

A central positive regulator of SAR signaling in *Arabidopsis* is NPR1 *(Non-expresser of Pathogenesis-Related genes 1*), also known as *Non-Immunity 1* [*NIM1*]). The gene is essential for transducing the salicylic acid (SA) signal to activate *Pathogenesis-Related* (*PR*) gene expression (Cao *et al.*, 1994; Dong, 2004). In addition, NPR1 is required by diverse immune signaling pathways, including basal defense, effector-triggered immunity (ETI) and induced systemic resistance (Rate & Greenberg, 2001; Shirano *et al.*, 2002; Spoel *et al.*, 2003; Pajerowska-Mukhtar *et al.*, 2013). NPR1 also mediates crosstalk between SA- and Jasmonic acid (JA)-mediated signaling pathways (Spoel *et al.*, 2003). The plant-specific transcription factor WRKY70 is identified as a common component downstream of NPR1 in both SA- and JA-mediated signal

pathways (Li *et al.*, 2004). *WRKY70* expression is activated by SA and repressed by JA.

NPR1 protein contains an ankyrin repeat domain and a broad complex, tramtrack, and bric-a`-brac/poxvirus and zinc-finger (BTB/ POZ) domain (Cao *et al.*, 1997; Aravind & Koonin, 1999). Since the first cloning of *Arabidopsis NPR1* in 1997 (Cao *et al.*, 1997), a significant amount of work has been done to understand the mode of NPR1 action. In the absence of infection, or at low concentration of SA, NPR1 predominantly exists as oligomers through intermolecular disulphide bonds and retained in the cytoplasm. After pathogen challenge, with elevated SA level, NPR1 converts to a monomeric state by reduction of the redox-sensitive disulphide bonds. It is then translocated to the nucleus, where NPR1 physically interacts with TGA-bZIP transcriptional factors and activates the expression of defense response genes (Mou *et al.*, 2003). Nuclear accumulation of NPR1 is needed for basal defense gene expression and resistance, whereas its subsequent turnover is required for establishing SAR (Spoel *et al.*, 2009). Two NPR1 paralogues, NPR3 and NPR4, are required to be the SA receptors (Fu *et al.*, 2012). Both NPR3 and NPR4 contain the BTB domain and ankyrin repeats, which are typical adaptors for CUL3 substrate. Either NPR3 or NPR4 can directly bind with SA and modulates their interactions with NPR1 that result in NPR1 degradation through CUL3 mediated ubiquitination (Fu *et al.*, 2012; Moreau *et al.*, 2012).

The monomeric state of NPR1 and the subsequent turnover and ubiquitination of the protein in *Arabidopsis* require a high-lever of SA often triggered by ETI. In plants, a superfamily of nucleotide-binding domain and leucine-rich repeat-containing proteins (NLRs) can recognize pathogen effectors and initiate ETI. Decades of studies on plant NLRs revealed two modes of actions, recognizing and signaling by itself, or formation of a heterogenous protein complex of NLR pairs often arranged in a head-to-head orientation where one acts as a sensor and the other as a transducer (Césari et al., 2014a; Williams et al., 2014; Saucet et al. 2015; Grund et al., 2019). Several of the sensor NLRs have been found to contain unconventional domains other than their conserved NLR multi-domains (Kanzaki et al., 2012; Césari et al., 2014b). These integrated domains (IDs)-containing NLRs are termed NLR-IDs of which the unusual integrated domains serve as decoys of effector targets in facilitating pathogen detection by the sensor NLR.

Given the pivotal role of NPR1 in defense signaling, studies have been conducted to investigate the role of *NPR1*-like genes in other plants. For example, a GhNPR1 was shown to play a key role in the SA-dependent systemic acquired resistance in Gladiolus (Zhong *et al.*, 2015). In wheat (*Triticum aestivum* L.), elevated *PR1* gene induction in transgenic lines carrying the *Arabidopsis* (*AtNPR1)* gene suggested a similar SA-dependent *NPR1*-mediated defense pathway exists in monocots. However, diversified functions of *NPR1*-like genes have also been revealed, suggesting the regulation of defense gene induction between dicots and monocots is quite different (Silverman *et al.*, 1995). In dicots, overexpression of *NPR1* orthologs in apple or grapevine has been shown to provide broad-spectrum resistance (Malnoy *et al.*, 2007; Le Henanff *et al.*, 2011). Overexpression of a rice NPR1 homolog led to constitutive activation of defense response and hypersensitivity to light (Chern *et al.*, 2005). Overexpression of *AtNPR1* in wheat enhanced resistance to *Fusarium graminearum*, a necrotrophic pathogen causing wheat head blight (Makandar *et al.*, 2006). A study in wheat-stripe rust pathogen *Puccinia striiformis* f. sp. *tritici* (*Pst*) interaction indicated that a *Pst* effector interact with wheat NPR1 during infection, implicating a role of wheat NPR1 during defense response to rust pathogens (Wang *et al.*, 2016).

There are three fungal pathogens from the genus Puccinia that cause wheat rust diseases, namely leaf rust (*P. triticina)*, stem rust (*P. graminis* f. sp. *tritici)*, and stripe rust (*Pst*). These three diseases combined can cause estimated annual losses of $2~5 billion to wheat production worldwide (http://www.usda.gov/nass) depending on the varieties grown and developmental stage when infection occurred. Wheat rust pathogens are biotrophs that only survive in living cells and sequester nutrients from their host via haustoria (Dodds *et al.*, 2004). HR is the most common phenotype observed among resistant wheat lines. In this study, we aimed to identify all the wheat homologs of *NPR1* (designated as *TaNPR1*) and explore their roles in the host defense response to rust pathogens. Our research revealed homeologous group 3 TaNPR1 proteins regulate transcription of SA-responsive *PR* genes. We also discovered a new mode of NPR1 action in wheat at the *Ta7ANPR1* locus through an NB-ARC-NPR1 fusion protein negatively regulating defense response to stem rust infection.

Materials and Methods

Plant materials

Alpowa (PI 566596), a soft, white, spring wheat cultivar, was obtained from the USDA National Plant Germplasm System (NPGS). Chinese Spring (CS) and CS+*Sr33* were from Dr. Evans Lagudah at Commonwealth Scientific and Industrial Research Organization (CSIRO). Chinese Spring nulli-tetra lines and deletion lines were provided by Dr. Bikram S. Gill at Kansas State University and Dr. Adam Lukazewski at UC Riverside. The EMS mutagenized Alpowa population was generated by the Giroux lab at Montana State University (Feiz *et al.*, 2009).

Mapping populations consist of 400 F_2 lines derived from a cross between the mutant Al^{R805Q} and Alpowa.

Sequence analysis

All BLASTs and the sequences downloads were conducted at either the National Center for Biotechnology Information at https://www.ncbi.nlm.nih.gov (Altschul et al., 1990) or the International Wheat Genome Sequencing Consortium (IWGSC) (IWGSC, 2014, 2018) (https://urgi.versailles.inra.fr/blast_iwgsc/blast.php). Softberry database FGENESH software (Solovyev et al., 2006) was used for gene prediction. DNASTAR software (www.dnastar.com) was used to analyze DNA sequences. InterProScan (http://www.ebi.ac.uk/InterProScan/), Pfam (http://pfam.xfam.org/) (El-Gebali et al., 2019), and PROSITE Scan (http://npsa-pbil.ibcp.fr) (Hulo et al., 2005) were used to predict the conserved domains and motifs. Multiple sequence alignments were created with ClustalW (http://www.ebi.ac.uk/Tools/msa/clustalw2/).

Plant growth conditions

For the race specificity screens, seeds were directly planted in 4-inch pots (5 seedlings/pot) containing SunGro Horticulture Sunshine mix (HeavyGardens Company, Denver, CO). Before inoculation, all the seedlings were grown in a growth room of the Plant Growth Center at Montana State University (PGC-MSU) under the following conditions: 22°C/14°C day/night temperatures and a 16-h photoperiod. Plants were watered every day and fertilized with Peters General Purpose Plant Food (Scotts-Miracle-Gro Company, Marysville, OH), at the concentration of 150 ppm

every other days.

Pathogens

The *Pgt* race QFCSC was used for the stem rust assay and was provided by Dr. Yue Jin from Cereal Disease Laboratory, USDA-ARS, St. Paul, MN. Leaf rust race *Pt* PBJJG was provided by Dr. Robert Bowden, USDA-ARS Manhattan, KS and is maintained at Montana State University. Stripe rust isolates were from the Plant Pathology Research Center at Yangling, Shaanxi, in China.

Pathogen inoculation

For leaf and stem rust tests, seedlings were inoculated with either *Pt* or *Pgt* at the 2-leaf stage. A video protocol detailing the process can be accessed at https://vimeo.com/48605764. Urediospores were mixed in Soltrol 170 Isoparaffin (Chempoint, Bellevue, WA) at a concentration of 0.5mg/mL. The suspension was sprayed onto the leaves using a Badger 350 airbrush gun and Propel propellant (Badger Air-Brush Company, Franklin Park, IL). The inoculated seedlings were then placed in a Percival I-60D dew chamber (Percival Scientific Inc., Perry, IA) with an ambient air temperature of 15-17°C for leaf rust and 19-22 °C for stem rust, respectively. After 24 hours of incubation, an additional 3 h high humidity and light intensity conditions were added for stem rust inoculated plants. All inoculated plants were then placed back in the growth chamber or greenhouse. Disease responses were assessed when rust symptoms were fully expressed on Alpowa 8-22 dpfi using the seedling 0-4 IT scale (Stakman *et al.*, 1962; McIntosh *et al.*, 1995). In detail, IT0: no visible uredia; IT; hypersensitive flecks; IT1: small uredia with necrosis; IT2: small to medium-sized uredia with green islands surrounded by necrosis; IT3: medium-sized uredia without necrosis; IT4: large-sized uredia without necrosis. The variations within each class are indicated by the use of "-" (less than average for the class) and "+" (more than average for the class).When variable reactions were observed, IT ranges are listed from lowest to highest.

Stripe rust inoculation and assessment

Stripe rust inoculations were conducted at the institute of plant pathology of Northwest A & F

University, China. Freshly collected uredospores were applied with a paintbrush to the surface of primary leaves of 7-day-old wheat seedlings. After inoculation, plants were incubated for 24 hours in dark in a 100% humidity dew chamber and were subsequently transferred to a growth chamber with a 16-hour photoperiod. Stripe rust infection types were assessed based on a 0 (immune)-9 scale (highest susceptible) (Line & Qayoum, 1992).

Quantification of pustule density on leaves

Infection types of wheat lines were quantified using ImageJ (http://rsb.info.nih.gov/ij) and presented by the average of the percentage of pustule area/leaf area from three leaves per treatment.

Virus-induced gene silencing (VIGS)

The BSMV vectors utilized in these experiments were obtained from Dr. Andrew O. Jackson at UC Berkeley. The fragments used to silence TaG7NPR1, TaG3NPR1 and Ta7ANPR1 were generated by PCR amplification from two synthesized oligonucleotides primers containing 10 overlapping base pairs at the 3' terminus (Table S1). Overlap Extension PCR amplification of dsDNA fragment using the program as follows：8 min at 95°C, followed by 34 cycles of 30 s at 95°C, 30 s at 32°C and 40S at 72°C, 2 min at 72°C. The target fragments were inserted into the modified γ vector ready for direct PCR cloning described by Campbell and Huang (Campbell & Huang, 2010). Infectious RNA transcripts were synthesized in vitro using T7 RNA polymerase (New England Biolabs, Ipswich, MA) from linearized α, β, and γ plasmids. The BSMV inoculum was prepared with 1μl of each of the in vitro transcription reactions and 22.5 μl inoculation FES buffer. The inoculum was then used to rub-inoculate the first leaf of the two-leaf stage plants. For simplicity, the BSMV-derived construct with no insert was named as γ00, and each BSMV silencing construct was named as γtarget. For example, a BSMV silencing construct carried a 185-bp fragment of the wheat PDS gene was named as γPDS. The concurrent silencing BSMV inoculum was made by combining the α:β:(γtarget1:γtarget2) transcripts in a 2:2:(1+1) ratio with excess FES. For example, silencing multiple genes both PDS and G7ANPR1, BSMV inoculum was made by combining an equimolar ratio of α, β, and (γPDS: γG7ANPR1) at a 2:2:2(1+1) ratio

with excess inoculation buffer (named as FES) containing a wounding agent.

Gene expression analysis by RT-qPCR and RNA-seq

The expression of the genes targeted for silencing was quantified by comparative QRT-PCR. Sampled tissues for the time-course study were immediately frozen in liquid nitrogen and stored at -80℃ prior to extraction of total RNA. Three independent biological replications were performed for each experiment. The time course of *G7ANPR1* gene expression was assessed by RT-qPCR. Wheat cultivar CS and CS+*Sr33*, was inoculated with the *Pgt* race QFCSC suspended in the inoculation buffer Soltrol 170 Isoparaffin (Chempoint, Bellevue, WA) and meanwhile, inoculation with Soltrol 170 Isoparaffin alone was used as mock control. Total RNA was isolated and treated with DNase I on column using the Qiagen RNeasy Plant Mini Kit (Qiagen, Valencia, CA) following the manufacturer's instruction. The quality and concentration of total RNA were assessed via agarose gels and $260/280_{ABS}$ measurements on a NanoDrop 2000 spectrophotometer (Thermo Fisher Scientific Inc., Wilmington, DE). Threshold values (Ct) generated from the CFX96 real-time PCR detection system (Bio-Rad, Hercules, CA) using iScript One-Step RT-PCR Kit with SYBR Green (Bio-Rad, Hercules, CA) following the manufacturers recommended protocol. We used gene-specific primers (Livak & Schmittgen, 2001) and relative gene expression $2^{-\Delta Ct}$ method for gene quantification. The amounts of RNA in each reaction were calculated using the average ΔCt normalized to three reference genes 18S rRNA, Actin and Glyceraldehyde 3-phosphate dehydrogenase (GAPDH). Primers specific for each gene are listed in Table S2. Each reaction was conducted in triplicate of the three biological replicates. So, relative expression of *G7ANPR1* gene is presented as expression level of this gene in the leaf rust inoculated plants relative to that in the control (buffer Soltrol170 Isoparaffin inoculated plants). Standard deviations were calculated among different biological replicates. Mean relative expressions were calculated using the ΔCt method between biological replicates ± standard deviation.

Wheat cultivar CS and CS+*Sr33*, were inoculated with BSMV inoculum combining an equimolar ratio of α, β, and γ transcripts suspended in the inoculation buffer containing a wounding agent

(FES). Meanwhile, inoculation with FES buffer alone was used as a mock control. All the leaf tissues snap-frozen in liquid nitrogen and stored at -80°C until the RNA isolation. The real-time PCR was conducted similarly with the time course stem rust inoculation study.

Expression abundance of *TaNPR1* homeologs were based on RNA sequence data already available in the Sequence Read Archive (SRA) of the National Center for Biotechnology Information (NCBI) via Kallisto software (Bray *et al.*, 2016). Sequence quality control checks were conducted via FastQC tool in interactive mode. Paired-end sequences were split using fastq-dump prior to transcript quantification. Wheat transcriptome data was downloaded from the IWGSC, indexed and reads are pseudoaligned. Transcript abundance was then quantified and recorded in transcript per million (tpm).

Mutant screen

The mutagenized population was generated by ethyl methane sulfonate (EMS) (Feiz *et al.*, 2009). The population was selfed and advanced to M_8 generation. The primers used in mutant identification were listed in Table S2.

For the A genome mutation screening, the A genome-specific primers G7A-MF + G7A-MR were designed to locate in the deletion variations among the A, B, and D genomes to ensure the A genome specificity (Fig. S1). To detect the A genome mutation, G7A-MF + G7A-MR used to screen the EMS induced population first. The PCR products were then purified using the QIAGEN gel purification kit (Valencia, CA), sequenced and compared. Firstly, the sequence from wild type Alpowa was compared with the *G7ANPR1* gene sequences of Chinese Spring from IWGSC, and then sequences from individual mutagenized lines were compared with the sequence of the wild type Alpowa for mutation identification.

SA/JA level analysis with the LC-MS

The extraction of SA/JA was according to Wang's method (Wang *et al.*, 2017). Frozen samples were then ground in liquid N_2 with mortar and pestle. An amount of about 200 mg fresh leaves was extracted with 750 µl mixture of $MeOH^{-}$:$H2O^{-}$:HOAc (90:9:1, v/v/v) and centrifuged for 1 min at 9,600g. The supernatant was collected and the extraction was repeated twice. Pooled

supernatants were dried in N_2, re-suspended in 1,000 µl of pure chromatographic grade MeOH, and finally filtered with a Millex- HV 0.22 µm filter from Millipore (Bedford, USA). Quantitation was done by the standard addition method by spiking control plant samples with SA and JA solutions (ranging from 50 to 1000 ng ml^{-1}), and extracting as described above. Analyses were carried out using an LC-30A+TripleTOF5600+ (AB SCIEX, Singapore) machine in Life Science Instrument Shared Platform of Northwest A & F University, China. Three biological replicates were carried out for each assay.

Results

Identification of wheat *NPR1* homologs

To identify *NPR1*-like genes in bread wheat (*Triticum aestivum*, L.), a cDNA of *NPR1*-like sequence, named as wheat chromosome 3 short arm NPR1 (W3SNPR1), was used as a probe to search its homologs via genomic blot 'Southern' hybridization. The W3SNPR1 shares a 99% sequence identity to another mRNA sequence deposited in NCBI (accession XM_020328292.1) predicted as a BTB/POZ and ankyrin repeat-containing NPR1-like protein amplified from *Aegilops tauschii* (D genome donor of bread wheat). Nine hybridization fragments were detected and the chromosome location of each fragment was determined using the wheat Chinese Spring (CS) nulli-tetrasomic (NT) lines (Fig.1a). In each NT line, a pair of chromosomes was missing and compensated by a pair of its homeologous chromosomes. For example, in N3AT3B, the two 3A chromosomes are missing and compensated by four 3B chromosomes. When a fragment is missing in N3AT3B compared to the rest of the NT lines, it suggests the missing fragment is located on 3A chromosomes. By such an analysis, two fragments were assigned to each of the chromosomes 3B, 3D and 7A and one was assigned to each of the chromosomes 3A, 4A (7B translocated region) and 7D (Fig.1a). The results revealed that all the wheat *NPR1* (referred as *TaNPR1* thereafter) homologs are located on six chromosomes of the two homeologous groups: 3A/3B/3D of group 3 (designated as *TaG3NPR1*) and 7A/4A/7D of group 7 (designated as *TaG7NPR1*). One *TaNPR1* homolog was found on chromosome 4A instead of 7B due to the ancient translocation between 4AL and 7BS in the tetraploid progenitor of hexaploid wheat (Liu *et*

al., 1992; Devos *et al.*, 1995).

The sequence of W3SNPR1 was then used to BLAST search the International Wheat Genomic Sequence Consortium (IWGSC-CS RefSeq v1.0) database. Nine NPR1-like proteins were identified (Notes S1). On chromosomes 3A, 3B and 3D (based on the prediction of FGENESH + genome annotation pipeline at Softberry.com), they each carry a gene that resembles a classical type of NPR1 protein with domains of BTB, ankyrin repeat and a highly conserved NPR1-like C terminal (Fig.1b). In addition, a gene encoding for an integrated protein of a kinase fused with NPR1 is found about 17~113 kb proximal to the classical TaG3NPR1 in the same orientation on each of chromosomes 3B and 3D. At the same homeologous locus of 3A there is only the C-terminal part of *NPR1*-like gene left, the sequence for protein kinase and most of the NPR1 domains are missing (Fig. 1b), explaining why only one fragment was detected on chromosome 3A in the 'Southern' result (Fig.1a). Additional search on the entire 3A sequences revealed no hits to the DNA sequence corresponding to the integrated kinase domain of the TaG3NPR1.

On 7A, 4A (7B) and 7D, each chromosome carries an NPR1 with additional domains. The N-terminal regions of the TaG7NPR1 proteins have domains of two consecutive DNA binding sites for MYC4 transcription factor and an NB-ARC (Fig.1c). In close proximity (650~3000bp) to each of the integrated TaG7NPR1, a gene encoding for a CC-like + an NB-ARC domain is found in the opposite orientation (Fig.1c). Similar *TaG7NPR1* genes in the same arrangement with a CC+NB-ARC were found in the A genome donor of *T. urartu* (http://plants.ensembl.org/Triticum_urartu/Info/Index) and *Ae. tauschii* (http://plants.ensembl.org/Aegilops_tauschii/Info/Index).

Silencing of the *TaNPR1* genes

After cloning of *Sr33* (Periyannan *et al.*, 2013), we sought to test the involvement of the *TaNPR1* genes in the *Sr33*-mediated defense response in wheat; we knocked down the endogenous *TaNPR1* genes in two wheat lines, CS and CS+*Sr33*, using a barley stripe mosaic virus-induced gene silencing (BSMV-VIGS) assay. Several silencing constructs were made for the assay. A

construct containing a 170-bp fragment conserved among the *TaG3NPR1* was used to silence all six *NPR1* homologs on group 3 chromosomes and labeled as BSMV:G3. Another distinct construct containing a 170-bp fragment conserved among the *TaG7NPR1* was used to silence the *NPR1* homologs on chromosomes 7A, 4A(7B) and 7D, and labeled as BSMV:G7. The sequences (Table S2) and locations (Notes S2, S3) of the primers are provided as supporting information. A construct carrying only the BSMV genome was used as a non-target control and labeled as BSMV:00, and a construct carrying a 183-bp phytoene desaturase (*PDS*) gene was used as a non-target control for the assay and labeled as BSMV:PDS. Three rounds of silencing assays were conducted: Round 1, silence all the homologs simultaneously via co-inoculation of two silencing constructs of BSMV:G3 and BSMV:G7 (labeled as BSMV:G3+G7); Round 2, silence only one group of *TaNPR1* at a time with inoculation of either BSMV:G3 or BSMV:G7; Round 3, silence a specific gene when needed. In each assay, CS and CS+*Sr33* seedlings inoculated with BSMV:00, BSMV:PDS and only the inoculation buffer (mock) were included as controls. Six days post BSMV (dpb) inoculations, and viral symptoms were visualized on the newly emerged leaves of plants inoculated with BSMV. At nine dpb, plants inoculated with BSMV:PDS started to show photo-bleaching phenotype, and plants inoculated with other BSMV constructs showed viral-symptom-free leaf segments, indicating BSMV induced gene silencing has been initiated. Three viral-symptom-free leaf segments were randomly sampled from plants inoculated with each targeting construct to check the expression level of the target genes through quantitative real-time PCR analysis with corresponding primers (Table S2). The results confirmed that about 30% reduction in relative expression of each *TaG3NPR1* and *TaG7NPR1* genes (Table S3). Stem rust pathogen *Pgt* race QFCSC was inoculated at 10 dpb. CS controls showed susceptible infection type scored as infection type (IT) 3 at 14 days post fungus inoculation (dpfi) (Fig. 2a). Resistant control CS+*Sr33* plants displayed a resistant phenotype score as IT1. A similar level of resistance was observed in CS+*Sr33* when both *TaG3NPR1* and *TaG7NPR1* were knocked down. Surprisingly, CS inoculated with either BSMV: G3+G7 or BSMV:G7 showed an enhanced level of resistance to the pathogen on the silenced leaf segments (Fig. 2a, b), suggesting knocking down *TaG7NPR1* genes enhanced CS resistance to the pathogen. However, when the six copies of

TaG3NPR1 were silenced in CS or CS+*Sr33*, infection types of silenced CS were as susceptible as their corresponding none-silenced or mock controls, and silenced CS+*Sr33* were as resistant as their controls, suggesting the *Sr33*-mediated resistance is *TaG3NPR1* independent (Fig. 2a, b).

TaG7NPR1 includes three homologs, *Ta7ANPR1*, *Ta4ANPR1* and *Ta7DNPR1*. To test which homeolog was vital for the enhanced resistance in CS, we aimed to silence each homeolog one at a time. However, the cDNAs of *Ta4ANPR1* and *Ta7DNPR1* are highly similar (Notes S3), we could not find a region to silence only one individual of the two, so the two genes were simultaneously silenced a construct labeled as BSMV:4A+7D. To silence *Ta7ANPR1* specifically, a region-specific to this gene was synthesized using two overlapped oligoes of G7AoligoF and G7AoligoR listed in Table S1 and was labeled as BSMV:7A. Only the *Ta7ANPR1* silenced plants showed enhanced resistance (Fig. 2a, b), whereas the plants silenced both *Ta4ANPR1+Ta7DNPR1* had no changes of infection types in response to *Pgt* QFCSC (Fig. 2a). Real-time PCR assays revealed the transcript abundance of each target gene in silenced CS plants was reduced about 20~41% from three biological replicates (Table S3). The experiments suggested that the *Ta7ANPR1* gene is the one negatively involved in the defense response to *Pgt* QFCSC. However, the resistance of CS in either *TaG7NPR1* or *Ta7ANPR1* silenced plants were better than the ones when both group 3 and 7 *TaNPR1* genes were silenced (Fig. 2a, b), suggesting a positive role of *TaG3NPR1* in defense against *Pgt* QFCSC.

Expression of *TaG7NPR1* post rust inoculations

Time course expressions of the three *TaG7NPR1* genes were analyzed using RNA seq datasets downloaded from NCBI. Notably, *Ta7ANPR1* was the only one among the three genes showing differential expression during stem rust infection in wheat plants (Fig. S2). Transcript abundances of *Ta4ANPR1 a*nd *Ta7DNPR1* were low and unchanged during the time courses post three rust inoculation in both compatible and incompatible interactions (Fig. S2).

To confirm the expression of *Ta7ANPR1* via real-time PCR, the transcript of the gene in wheat line CS was analyzed with three pairs of overlapped primers. In the absence of pathogen infection conditions, only a 5,785-bp cDNA (labeled as Ta7ANPR1 cDNA-1) was amplified

(Fig. 3). The protein encoded by this mRNA has only 881 amino acids with a stop codon appearing after exon 3, resulting in a short protein without any signature domains of NPR1 (Fig. 3). To understand why the NPR1 domain was absent from the transcript, we investigated possible alternative splicing at the locus using the primers flanking the stop codon and two RNA samples of CS grown under biotic-stressed conditions such as rust/virus infection. An additional fragment was discovered from CS RNA extracted from leaf tissues 24 hours after inoculation with either stripe rust or barley stripe mosaic virus (Fig. 4a) or Cadenza RNA 24 hours after stem rust inoculation (Fig. 4b). This alternative spliced transcript of *Ta7ANPR1* has the intron (including the stop codon) that was retained between exons 3 and 4 in the cDNA-1 spliced out and translates to a protein of 1,437 amino acids with fused domains of NB-ARC and NPR1 (Fig. 3). The same alternative spliced transcript was also identified from RNA-seq data generated from a pair of wheat *Lr47*-cultivar 'Scholar' near isogeneic lines (NILs) post leaf rust pathogen inoculation (Fig. 4c). Interestingly, the transcript encoding for the protein without NPR1 domains was upregulated about eight-fold in the susceptible NIL (Scholar/-*Lr47*), whereas the levels of the two types of *Ta7ANPR1* transcripts were about the same in the resistant NIL (Scholar/+*Lr47*) and doubled the expressions at 2 days post *Pt*-inoculation (Fig. 4c).

The transcript abundances of the two mRNA isoforms encoding for NB-ARC (the long isoform) and NB-ARC-NPR1 (the short isoform) were quantitatively measured via real-time qRT-PCR in Cadenza during the time course of *Pgt* TPMKC (Cadenza was susceptible) inoculation. Two sets of primers were designed as shown in Fig. 4b. One pair is flanking the borders of the spliced-out region (925 bp), the other pair is inside the spliced fragment. During qRT-PCR, we set up the program with 20 second extension time to only allow ~200-bp fragment amplified. Under the given conditions, the primers flanking the 925-bp alternatively spliced region can only be amplified from the short isoform when the 925-bp fragment is spliced out.

Meanwhile, the primers located inside the spliced fragment can only be amplified from the long intron-retention mRNA. The transcript abundance of the two isoforms could be measured in the same RNA sample with two rounds of PCR setups. The short NB-ARC-NPR1 isoform was undetectable in the absence of the rust infection (Fig. 4b). However, once the NB-ARC-NPR1

mRNA was detectable at 1 dpi, the two isoforms had a similar level expression during the course of *Pgt* TPMKC infection (Fig. 4b).

Identification of *Ta7ANPR1* Mutants

Six independent mutants of *Ta7ANPR1* were identified from two spring wheat backgrounds, three from 'Alpowa' and three from 'Cadenza'. The Alpowa mutants were identified by a set of primers, G7A-MF1+G7A-MR1 (Table S2), specifically designed for *Ta7ANPR1* after screening an ethyl methane sulfonate (EMS) mutagenized Alpowa population (Feiz *et al.*, 2009). The specificity of the primers was verified on three group 7 NT lines. A 508-bp fragment was amplified from N7BT7D and N7DT7B but not from N7AT7D (Fig. S1), confirming that the primers are specific to amplify *Ta7ANPR1*. After screening 576 individuals from the mutagenized population, a total of three mutations between the primers were identified. One mutant is a G to A transition resulting in a codon of GGG to GAG but is synonymous at the amino acid level. Of the other two mutants each one had a missense mutation on *Ta7ANPR1,* resulting in a S to L at location 736 (named as Al^{S736L}) and an R to Q at location 805 (Al^{R805Q}). Both mutations were located within the NB-ARC domain (aa 525-814). The mutants were then tested with *Pgt* TPMKC, along with CS and Alpowa as susceptible controls, and CS+*Sr33* as a resistance control. As expected, the mutant with a silent mutation had a similar infection type as CS and Alpowa and so did Al^{S736L} (data not shown). Al^{R805Q} was resistant to the pathogen (Fig. 5a).

To confirm the new resistance of Al^{R805Q} was due to the mutation, we made a cross between the mutant (as a male parent) and the wild type Alpowa. Ten F_1 individuals were tested with *Pgt* TPMKC and showed a susceptible infection phenotype at 14 days post-inoculation, whereas Al^{R805Q} was highly resistant and wild type Alpowa was susceptible (Fig. 5a). The ten F_1 individuals were bagged and selfed to produce F_2 seeds. Four hundred F_2 were screened with *Pgt* TPMKC at the seedling stage, the segregation of resistant to susceptible fits 1:3 ratio. Seventy-five susceptible and 21 resistant individuals were sampled to amplify the region of mutation at *Ta7ANPR1* via PCR using the gene-specific primers. The sequence data confirmed

the new resistance completely co-segregated with the SNP between Al^{R805Q} and Alpowa.

The three mutants from wheat cultivar 'Cadenza' were identified from the wheat-TILLING database (Krasileva et al., 2018) (https://www.seedstor.ac.uk/shopping-cart-tilling.php) using *Ta7ANPR1* sequence as a query. The database has more than 50 lines carrying a mutation on the *Ta7ANPR1* gene in a heterozygous state. We requested three lines Cd^{A529E}, Cd^{M357I}, and Cd^{L1224R}, and selected homozygous mutations of each line after genotyping. The homozygous Cd^{A529E} and Cd^{M357I} mutants showed resistance to *Pgt* TPMKC (Fig. 5b), whereas Cd^{L1224R} (mutation located in the DUF3420 unknown domain of the NPR1 portion) was as susceptible as the wild type (Data not shown).

Homozygous mutant Al^{R805Q} was also tested with *Pt* PBJJG and two *Pst* races. The mutant was as susceptible as the wild type to *Pt* PBJJG (Fig. 5c) and *Pst* race CYR31 (Fig. 5d), but was less susceptible to *Pst* CYR23 than the wild type (Fig. 5e). The infection type of each genotype is also quantified as a percentage of pustule area/leaf area (Fig. 5f). These results suggested the resistance of the mutant was rust pathogen-species specific and race-specific.

Levels of SA/JA and *PR* genes when the *TaG3NPR1* genes were down-regulated

A known function of NPR1 is associated with SA-mediated signaling pathway, and no visible infection type changes were observed with *Pgt* inoculation when *TaG3NPR1* were down-regulated, so we decided to measure the levels of SA/JA and five *PR* genes in CS leaf segments where the six copies of *TaG3NPR1* were silenced, and post-*Pst* inoculation. Leaf segments of the same stage as the silenced ones from CS seedlings without any treatments (mock) or treated with BSMV virus alone (BSMV:00) were used as controls. At ten days post BSMV inoculation, six viral-symptom-free leaf segments were sampled from each treatment. Each grounded leaf sample was divided into three portions; one of each was used for RNA extraction, SA and JA measurements. After confirming the *TaG3NPR1* levels were reduced at least 30% compared to the BSMV:00 control, the top three best *TaG3NPR1*-silenced samples (Fig. S3a) were selected for further tests of SA, JA and the *PR* genes. We observed significant high levels of SA in the leaves with BSMV-inoculations (Fig. S3b) compared with the mock

control. However, the levels of three SA-mediated *PR* genes were similar among the high-SA and low-SA samples (Fig. S3d). When we measured the SA/JA and *PR* genes at 24 hours post-*Pst* inoculation (hpi), the level of SA slightly reduced compared with the levels without *Pst,* but the three *PR* genes were significantly increased (Fig. S3d). We learned from these observations that high-SA level does not equal to high *PR1* level, but the expression of *PR1* did associate with a certain level of SA concentration, suggesting SA was essential for *PR1* expression. SA alone was not sufficient to achieve high levels of *PR1, PR2* and *PR5*. Interestingly, at 24 hpi, the SA levels detected in *TaG3NPR1* silenced leaves (Fig. S3b) were significantly higher than that in the non-silenced leaves, but the levels of *PR1, PR2,* and *PR5* genes were significantly lower than the levels in the non-silenced leaves (Fig. S3d), suggesting some of the *TaG3NPR*1 genes were required for the SA-mediated *PR* gene expression.

In contrast, the level of JA in BSMV:00 control was significantly lower than those from the mock and *TaG3NPR1* silenced leaves without *Pst* inoculation (Fig. S3c); no differences in the levels of *PR3* and *PR10* genes were detected among the treatments (Fig. S3e). Post-*Pst* inoculation, the levels of JA were slightly decreased at 24 hpi (Fig. S3c), but *PR3* expression level increased, and the level was significantly higher in the *TaG3NPR1* silenced leaves than that in non-silenced controls (Fig. S3e).

Expression of *TaG3NPR1* post-*Pst*-inoculation

It was impossible to silence each *TaG3NPR1* gene individually because of their high level of cDNA similarity (Notes S2). We, therefore, explored their expression levels post-*Pst*-inoculation using the RNA-seq datasets generated from a *Yr5* line in Avocet background and a highly stripe rust susceptible wheat variety "Vuka" (Dobon et al., 2016) downloaded from NCBI. Interestingly, four of the six *TaG3NPR1* genes have detectable transcripts (Fig. S4). The *Ta3ANPR1* and *Ta3BNPR1* genes have similar expression profiles, upregulated at 1 dpi in the *Yr5* resistant line, and no changes in the susceptible line over the time course. The two kinase-*TaG3NPR1* fusion genes in 3B and 3D also have similar profiles with an increased expression in the resistant line starting at 3 dpi (Fig. S4). The expression profiles of the four

TaG3NPR1 genes led us to infer that *Ta3ANPR1* and *Ta3BNPR1* are more likely to be responsible for regulating SA-responsive genes based on the timing of their upregulation.

Transcript abundance of *PR* genes when the *Ta7ANPR1* gene was knocked down or knocked out

The same five *PR* genes were measured when the *Ta7ANPR1* gene was knocked down under two conditions, 48 hours post-inoculation (hpi) with *Pst* CYR32 or without *Pst* inoculation. All five genes had relatively low expression without rust, but *PR2* and *PR3* genes had even lower expressions in silenced leaves (Fig. S5a) than those in control (Fig. S5b, c). Three of the five *PR* genes (*PR1*, *PR2,* and *PR3*) showed a significant up-regulation at 48 hpi (Fig. S5b, c). All except *PR3* had a similar level of increase between silenced and none-silenced leaves. The up-regulation of *PR3* was affected when the *Ta7ANPR1* gene was down-regulated, suggesting a decisive role of *Ta7ANPR1* to this JA-responsive *PR* gene.

To explore why the mutations on *Ta7ANPR1* enhanced resistance to stem rust, we also analyzed the five *PR* genes in the two mutants Cd^{A529E} and Al^{R805Q} in the absence of pathogens. All five *PR* genes had low expression levels between the mutant Al^{R805Q} and the wild-type Alpowa (Fig. S6). The mutant Cd^{A529E} also had low expression levels in four of the five *PR* genes (Fig. S6) except the *PR10* level in Cd^{A529E} was significantly higher than that in the wild-type Cadenza (Fig. S6).

Because the *PR1* gene was undetectable in Cadenza and the mutant, and *PR10* expression was different between the two lines without the pathogen, we measured the transcript abundances of the two *PR* genes post-*Pgt* TPMKC at 5 time points (Fig. S7). *PR1* became detectable at 1 dpi but at very low levels until 5 dpi in both Cd^{A529E} and Cadenza (Fig. S7a). A different pattern was observed with *PR10* with a relatively high base-level expression; mutant Cd^{A529E} had an upregulated *PR10* expression during 1~2 dpi and then gradually returned to the base-level from 3 dpi (Fig. S7b). In contrast, Cadenza had a low *PR10* level during the early time points (1~2 dpi) and slowly increased the level at later time points (3~5 dpi) (Fig. S7b).

Discussion

A requirement of NPR1 in wheat defense response to *Puccinia* is selective

Bread wheat has nine homologs of the NPR1-like gene in the genome. Three of them, named as wNPR1 by Cantu et al. (Cantu *et al.*, 2013), are the three classical types of *NPR1*-like genes in homeologous group 3 chromosomes (Fig. 1b) with similar functional domains as the *Arabidopsis* AtNPR1. wNPR1 has a similar mode of action as the AtNPR1, interacting with a TGA transcription factor for the transduction of the SA signal (Cantu *et al.*, 2013). During wheat-*Puccinia striiformis* interaction, the wNPR1 was targeted by a stripe rust effector protein PNPi (for *Puccinia* NPR1 interactor) (Wang *et al.*, 2016). The PNPi competes with wNPR1 for the interaction with TGA2.2 and reduced pathogenesis-related gene expression (Wang *et al.*, 2016). Similarly, when the *TaG3NPR1* gene was knocked down with a BSMV:G3NPR1 construct in our study, we found three SA-mediated *PR* genes (*PR1, PR2* and *PR5*) had significantly lower expression levels compared to the control (Fig. S3f). These results suggested that the *TaG3NPR1* was involved in wheat defense response against stripe rust as the classical *NPR1* gene for transducing the SA signal to activate *PR* gene expression (Cao *et al.*, 1994; Dong, 2004). However, down-regulating *TaG3NPR1* did not alter the infection type phenotype of the *Sr33*-mediated stem rust resistance (Fig. 2), suggesting defense response to stem rust conferred by *Sr33* did not require TaG3NPR1. Similarly, NPR1 is not always required in resistance in *Arabidopsis*. An NPR1-independent resistance to a bacterial pathogen *Pseudomonas syringae* pv. *maculicola* and an oomycete *Peronospora parasitica* were identified in *Arabidopsis* (Li *et al.*, 2001). This pathway bypasses NPR1 but requires SA and is an EDS1-mediated pathway (Li *et al.*, 2001). Our study suggested *Sr33*-mediated resistance is NPR1-independent, but it should not be generalized to imply that NPR1 is not required for immunity to stem rust based on only one gene. Clearly, more studies on other *Sr* genes are necessary to draw such a conclusion. The function of *AtNPR1* in other plant species may not be the same as observed in *Arabidopsis*. *AtNPR1* in rice has a similar function of its *NPR1* homolog as it could enhance resistance against bacterial pathogen *Xanthomonas oryzae* pv. *oryzae* (Xoo) (Chern *et al.*, 2005), but was more susceptible to herbivore attack (Yuan *et al.*, 2007). *AtNPR1*-expressing wheat was resistant to Fusarium head blight (Makandar *et al.*, 2006), but was more susceptible to Fusarium seedling blight (Gao *et al.*, 2013).

Given the importance of NPR1 in host defense, the protein also becomes a target of pathogens. In rice, the NPR1 interacting protein NRR negatively regulates defense response to Xoo. In brief, NPR1 is an important component in plant defense, but its involvement in SA defense signaling is not a universal phenomenon.

NPR1 proteins with integrated domains in the wheat genome

Besides the classical type of *NPR1*, five homologs of *NPR1*-like gene in the bread wheat genome occur as gene fusions with exogenous domains such as a protein kinase (Fig. 1b) or an NB-ARC domain of the most common plant immune receptors (Fig. 1c). The IWGSC and the EnsemblPlants databases have the sequences at all loci but the search tools fail to reveal them as fused NPR1 proteins. It was only in a recent study by Bailey et al. (2018) where three NB-ARC-NPR1 fused proteins in hexaploid wheat based on gene predictions were reported (Bailey *et al.*, 2018). Our findings back up the prediction. A possible reason why the NPR1 fused proteins were overlooked may be attributed to the findings in our study where the mRNA of the *Ta7ANPR1* gene in the absence of pathogen infection has a stop codon before the sequences coding for the NPR1-like domains (Fig. 4). Consequently, the gene was predicted only as an NB-ARC containing protein. The NPR1 proteins with integrated domains are produced only when the gene is alternatively spliced under certain stresses, for example, biotic stresses (Fig. 4a). Because the sequences of *TaG7NPR1* in bread wheat can be traced to its diploid ancestors (alternatively spliced variants annotated for the diploid D genome as AETGV20038900.1, AETGV20038900.2, and AETGV20038900.3), it indicated the NB-ARC-NPR1 fused protein already existed in the diploid donor species of bread wheat. Evolutionary events to create this NB-ARC-NPR1 fusion and selection sweeps have maintained these NPR1 fused proteins, implying the benefits of these proteins for wheat. Several pieces of findings suggest that NPR1 might contribute to defense against pathogens. The classic TaG3NPR1 proteins have been shown to be involved in stripe rust resistance and a target of the pathogen (Wang *et al.*, 2016). It raises the possibility that the NPR1 domain of the Ta7ANB-ARC-NPR1 is used as a decoy to monitor

the wNPR1. The organization of the group 7 *NB-ARC-NPR1* genes in a head-to-head orientation with another *NB-ARC*-like gene (Fig. 1c) is indicative of some disease resistance gene pairs that require sensing and signaling partners to confer resistance function, for example, the *RRS1/RPS4* pair (Narusaka *et al.*, 2009) and the *Pi5-1/Pi5-2* pair (Lee *et al.*, 2009).

The negative regulation of Ta7ANBS-NPR1 is specific

The function of the Ta7ANB-ARC-NPR1 fusion protein does not appear to enhance a general defense to all pathogens because the mutants showed resistance to stem rust (Fig. 5a, b), stripe rust CYR23 (Fig. 5e) but not to leaf rust PBJJG (Fig. 5c) and stripe rust CYR31 (Fig. 5d). It appeared the mutations lift the suppression on specific rust resistance genes. Among the six mutants identified, we only identified one mutant that has a mutation in the NPR1 portion of the fusion protein, the resistant mutants all have a mutation located in the NB-ARC region of the gene. We consider the resistance against *Pgt* TPMKC in the mutants was due to the sequence changes in the NB region of the protein that altered the formation of the R protein complex. The resulting activated defense was hypothesized as mutation-based rather than recognition-based (Fig. 6a). The biotic stress caused by the rust infection triggered the alternative splicing at the *Ta7ANPR1* locus. It is likely the NLR-NPR1 fusion protein may not recognize *Pgt* TPMKC in the wheat cultivars CS and Cadenza because these two wheat lines were susceptible to the pathogen. The mutation-based preformed defense was only sufficient against some rusts but not others, suggesting other components of the defense pathway might be the subjects of pathogen attack. Our previous study at the *MNR220* locus also revealed that different rust pathogens recognized by the same *R* gene locus activated different *PR* genes, suggesting different signaling pathways were used (Zhang et al., 2018). A wide range of NLR fusion IDs suggested the complexity of the exquisite nature of the plant pathogen surveillance systems and different defense signaling to cope with the highly sophisticated pathogen invasion strategies to stay healthy.

Alternative splicing has been reported to be associated with stresses, including abiotic and biotic stresses (Jordan *et al.*, 2002; Zhang & Gassmann, 2007; Filichkin *et al.*, 2015). Numerous

TIR-NB-LRR and CC-NB-LRR plant R proteins have alternative isoforms (Ayliffe *et al.*, 1999; Gassmann *et al.*, 1999; Dinesh-Kumar & Baker, 2000; Dodds *et al.*, 2001; Jordan *et al.*, 2002). The location of the alternative splicing, so far, has only been seen between the sequence coding for NB and LRR domains (Jordan *et al.*, 2002). In some cases, not only the presence of the alternative isoforms of the gene but also their ratio is crucial for active resistance against pathogen attack (Dinesh-Kumar & Baker, 2000). In other cases, for example, *L6*, although an alternative form of *L6* was detected, no functional relevance could be assigned (Dodds *et al.*, 2001). Our studies revealed that the alternative splicing from a locus of 7A is regulated by both the host and pathogen (Fig. 4b, c). The isoform of the Ta7ANB-NPR1 fusion protein is promoted by the host and suppressed by the pathogen during the interaction, suggesting alternative splicing is one of the strategies used by both host and pathogen during an interaction.

Expression profiles of the five *PR* genes in *Ta7ANPR1* knocked down and knocked out lines seemed to reveal the same thing that *Ta7ANPR1* affected *PR3* expression (Fig. S5c; S6, S7a, b). These observations might suggest that the Ta7ANPR1 protein has both negative and positive functions. The negative regulatory role of the fusion protein is more likely located in the NB-ARC region (Fig. 6a), and the NPR1 domains may be involved in regulating some *PR* gene expression. There are two Helix-Turn-Helix (HTH) motifs in both NB-ARC and NB-ARC-NPR1 proteins (Fig. 1c). Since the HTH motif has a G-box DNA binding property, we speculate that the function of these HTH motifs might be associated with MYC2 with negative regulation of *PR3* and *PR10*. Upregulated expressions of two JA-responsive *PR* genes (*PR3* and *PR10*) in the *Ta7ANPR1* mutant (Fig. S6), suggesting repression of JA-mediated transcription in the wild-type. However, if down-regulating Ta7ANPR1 proteins also affected *PR3* expression (Fig. S5c), suggesting the requirement of Ta7ANPR1. Thus, we hypothesize a scenario in which the Ta7ANB-ARC-NPR1 protein competes with the Ta7ANB-ARC protein to bind the G box DNA of the regulated genes. Degradation of the Ta7ANB-ARC-NPR1 protein by NPR1 directed-ubiquitination releases the negative regulation. Further investigations on the association between Ta7ANB-ARC-NPR1 and MYC2 and their association with the G box DNA of the two *PR* genes are required to substantiate the claim.

Potential roles of TaNPR1 proteins during wheat-rust interactions

We believe that the history of the wheat-rust co-evolution and the complexity of their interactions are partially revealed by the results of ours and others. The pathogens have to be able to sabotage the host defense systems without being detected to be successful. Any components in the host defense pathways could be a subject of the pathogen target. We hypothesize the potential roles of *TaNPR1*-like genes during wheat-rust interactions, as illustrated in Fig. 6b. From the angle of the rusts, the pathogens could include targeting TaNPR1 as one of the strategies or not, namely the "Yes" or the "No" group. Wheat infection types will reflect the effectiveness of the host defense in terms of pathogen detection and defense signaling. Wheat plants that have neither an effective detection system nor components for inducing defense signals will be susceptible to the pathogens. Resistant wheat to the "Yes" group of rusts are postulated to have an alternative defense signaling pathway that is independent of TaNPR1 to overcome the rust invasion strategy of attacking TaNPR1. A more advanced host may include using TaNPR1 as a decoy in the detection and have an alternative pathway bypass TaNPR1 once the integrity of the NPR1 component is compromised by the pathogens.

Acknowledgments

Xiaojing Wang wishes to thank the National Key Research and Development Program of China (No.2018YFD0200405) and the Shaanxi Provincial Postdoctoral fund (2017). Hongtao Zhang and Bernard Nyamesorto wish to thank the NSF BREAD program (Grant No. IOS-0965429) for financial support. The authors thank Dr. Hikmet Budak for help with the analysis of the *Ta7ANPR1* alternative isoform, and Dr. Michael Giroux for the use of his Alpowa mutagenesis population. We also would like to thank Northwest A&F University Life Science Research Core Services for letting us use the equipment for SA/JA tests.

Author contributions

X.W., Z.K., E.L., and L.H. planned and designed the research; X.W., H.Z., Y.L., X.M., B.N., and F.W. performed the experiments and analyzed data; X.W., E.L. and L.H. wrote the manuscript;

X.W., H.Z., and B.N contributed equally to this work.

References

Altschul SF, Gish W, Miller W, Myers EW, Lipman, DJ. 1990. "Basic local alignment search tool." *Journal of Molecular Biology* **215:**403-410.

Aravind L, Koonin EV. 1999. Fold prediction and evolutionary analysis of the POZ domain: Structural and evolutionary relationship with the potassium channel tetramerization domain. *Journal of Molecular Biology* **285**(4): 1353-1361.

Ayliffe MA, Frost DV, Finnegan EJ, Lawrence GJ, Anderson PA, Ellis JG. 1999. Analysis of alternative transcripts of the flax *L6* rust resistance gene. *Plant Journal* **17**(3): 287-292.

Bailey PC, Schudoma C, Jackson W, Baggs E, Dagdas G, Haerty W, Moscou M, Krasileva KV. 2018. Dominant integration locus drives continuous diversification of plant immune receptors with exogenous domain fusions. *Genome Biology* **19**. 23. https://doi.org/10.1186/s13059-018-1392-6.

Bray NL, Pimentel H, Melsted P, Pachter L. 2016. Near-optimal probabilistic RNA-seq quantification. *Nature Biotechnology* **34**(5): 525-527.

Campbell J, Huang L. 2010. Silencing of multiple genes in wheat using Barley stripe mosaic virus. *Journal of Biotech Research* **2**(1): 12-20.

Cantu D, Yang BJ, Ruan R, Li K, Menzo V, Fu DL, Chern M, Ronald PC, Dubcovsky J. 2013. Comparative analysis of protein-protein interactions in the defense response of rice and wheat. *Bmc Genomics* **14**: 166.

Cao H, Bowling SA, Gordon AS, Dong XN. 1994. Characterization of an *Arabidopsis* mutant that is nonresponsive to inducers of systemic acquired-resistance. *Plant Cell* **6**(11): 1583-1592.

Cao H, Glazebrook J, Clarke JD, Volko S, Dong XN. 1997. The *Arabidopsis* NPR1 gene that controls systemic acquired resistance encodes a novel protein containing ankyrin repeats. *Cell* **88**(1): 57-63.

Chern M, Fitzgerald HA, Canlas PE, Navarre DA, Ronald PC. 2005. Overexpression of a rice NPR1 homolog leads to constitutive activation of defense response and hypersensitivity to light. *Molecular Plant-Microbe Interactions* **18**(6): 511-520.

Césari S, Kanzaki H, Fujiwara T, Bernoux M, Chalvon V, Kawano Y, Shimamoto K, Dodds P, Terauchi R, Kroj T. 2014a. The NB-LRR proteins RGA4 and RGA5 interact functionally and physically to confer disease resistance. *EMBO J.* **33:**1941-1959.

Césari S, Bernoux M, Moncuquet P, Kroj T, Dodds PN. 2014b. A novel conserved mechanism for plant NLR protein pairs: The "integrated decoy" hypothesis. *Frontiers in Plant Science* **5:** 606

Devos KM, Dubcovsky J, Dvorak J, Chinoy CN, Gale MD. 1995. Structural evolution of wheat chromosomes 4a, 5a, And 7b and its impact on recombination. *Theoretical and Applied Genetics* **91**(2): 282-288.

Dinesh-Kumar SP, Baker BJ. 2000. Alternatively spliced *N* resistance gene transcripts: Their possible role in tobacco mosaic virus resistance. *Proceedings of the National Academy of Sciences of the United States of America* **97**(4): 1908-1913.

Dobon A, Bunting DCE, Cabrera-Quio LE, Uauy C, Saunders DGO. 2016. The host-pathogen interaction between wheat and yellow rust induces temporally coordinated waves of gene expression. *Bmc Genomics* **17:** 380-380.

Dodds PN, Lawrence GJ, Catanzariti A-M, Ayliffe MA, Ellis JGJTPC. 2004. The Melampsora lini *AvrL567* avirulence genes are expressed in haustoria and their products are recognized inside plant cells. *Plant Cell* **16**(3): 755-768.

Dodds PN, Lawrence GJ, Ellis JG. 2001. Six amino acid changes confined to the leucine-rich repeat beta-strand/beta-turn motif determine the difference between the P and P2 rust resistance specificities in flax. *Plant Cell* **13**(1): 163-178.

Dong XN. 2004. NPR1, all things considered. *Current Opinion in Plant Biology* **7**(5): 547-552.

El-Gebali J, Mistry A, Bateman SR, Eddy A, Luciani SC, Potter M, Qureshi LJ, Richardson GA, Salazar A, Smart ELL, Sonnhammer L, Hirsh L, Paladin D, Piovesan SCE,

Tosatto RD. 2019. The Pfam protein families database in 2019. *Nucleic Acids Research.* doi: 10.1093/nar/gky995

Feiz L, Beecher BS, Martin JM, Giroux MJ. 2009. In planta mutagenesis determines the functional regions of the wheat puroindoline proteins. *Genetics* **183**(3): 853-860.

Filichkin S, Priest HD, Megraw M, Mockler TC. 2015. Alternative splicing in plants: directing traffic at the crossroads of adaptation and environmental stress. *Current Opinion in Plant Biology* **24**: 125-135.

Fu ZQ, Yan SP, Saleh A, Wang W, Ruble J, Oka N, Mohan R, Spoel SH, Tada Y, Zheng N, et al. 2012. NPR3 and NPR4 are receptors for the immune signal salicylic acid in plants. *Nature* **486.** 228–232.

Gao CS, Kou XJ, Li HP, Zhang JB, Saad ASI, Liao YC. 2013. Inverse effects of *Arabidopsis NPR1* gene on fusarium seedling blight and fusarium head blight in transgenic wheat. *Plant Pathology* **62**(2): 383-392.

Gassmann W, Hinsch ME, Staskawicz BJ. 1999. The *Arabidopsis RPS4* bacterial-resistance gene is a member of the TIR-NBS-LRR family of disease-resistance genes. *Plant Journal* **20**(3): 265-277.

Grund E, Tremousaygue T, Deslandes L. 2019. Plant NLRs with integrated domains: unity makes strength. *Plant Physiology.* **179:** 1227-1235.

Hulo N, Bairoch A, Bulliard V, Cerutti L, De Castro E, Langendijk-Genevaux PS, Pagni M, Sigrist CJA. 2006. The PROSITE database. *Nucleic Acids Research.* **34.** D227-230.

International Wheat Genome Sequencing Consortium. 2014. A chromosome-based draft sequence of the hexaploid bread wheat (*Triticum aestivum*) genome. *Science.* **345.** 286.

International Wheat Genome Sequencing Consortium. 2018. Shifting the limits in wheat research and breeding using a fully annotated reference genome. *Science.* **361,** 661.

Jordan T, Schornack S, Lahaye T. 2002. Alternative splicing of transcripts encoding Toll-like plant resistance proteins-what's the functional relevance to innate immunity? *Trends Plant*

Science **7**(9): 392-398.

Kanzaki H, Yoshida K, Saitoh H, Fujisaki K, Hirabuchi A, Alaux L, Fournier E, Tharreau D, Terauchi R. 2012. Arms race co-evolution of *Magnaporthe oryzae AVR-Pik* and rice *Pik* genes driven by their physical interactions. *Plant Journal* **72:** 894–907

Le Henanff G, Farine S, Kieffer-Mazet F, Miclot AS, Heitz T, Mestre P, Bertsch C, Chong J. 2011. Vitis vinifera VvNPR1.1 is the functional ortholog of AtNPR1 and its overexpression in grapevine triggers constitutive activation of *PR* genes and enhanced resistance to powdery mildew. *Planta* **234**(2): 405-417.

Lee S-K, Song M-Y, Seo Y-S, Kim H-K, Ko S, Cao P-J, Suh J-P, Yi G, Roh J-H, Lee SJG. 2009. Rice *Pi5*-mediated resistance to *Magnaporthe oryzae* requires the presence of two coiled-coil–nucleotide-binding–leucine-rich repeat genes. *Genetics* **181**(4): 1627-1638.

Li J, Brader G, Palva ET. 2004. The WRKY70 transcription factor: A node of convergence for jasmonate-mediated and salicylate-mediated signals in plant defense. *Plant Cell* **16**(2): 319-331.

Li X, Clarke JD, Zhang YL, Dong XN. 2001. Activation of an *EDS1*-mediated *R*-gene pathway in the snc1 mutant leads to constitutive, NPR1-independent pathogen resistance. *Molecular Plant-Microbe Interactions* **14**(10): 1131-1139.

Line RF, Qayoum A. 1992. Virulence, aggressiveness, evolution and distribution of races of *Puccinia striiformis* (the cause of stripe rust of wheat) in North America, 1968-87. *Technical bulletin-United States Department of Agriculture.* **1788:** 44.

Liu C, Atkinson M, Chinoy C, Devos K, Gale M. 1992. Nonhomoeologous translocations between group 4, 5 and 7 chromosomes within wheat and rye. *Theoretical and Applied Genetics* **83**(3): 305-312.

Livak KJ, Schmittgen TD. 2001. Analysis of relative gene expression data using real-time quantitative PCR and the $2^{-\Delta\Delta CT}$ method. *Methods.* **25**(4): 402-408.

Makandar R, Essig JS, Schapaugh MA, Trick HN, Shah JJMP-MI. 2006. Genetically engineered resistance to Fusarium head blight in wheat by expression of *Arabidopsis*

NPR1. *Molecular Plant-Microbe Interactions* **19**(2): 123-129.

Malnoy M, Jin Q, Borejsza-Wysocka E, He S, Aldwinckle H. 2007. Overexpression of the apple MpNPR1 gene confers increased disease resistance in Malus× domestica. *Molecular Plant-Microbe Interactions* **20**(12): 1568-1580.

McIntosh RA, Wellings CR, Park RF. 1995. *Wheat rusts: an atlas of resistance genes*: CSIRO Publishing. Clayton, Victoria, Australia.

Moreau M, Tian M, Klessig DF. 2012. Salicylic acid binds NPR3 and NPR4 to regulate NPR1-dependent defense responses. *Cell Research* **22**(12): 1631.

Morel JB, Dangl JL. 1997. The hypersensitive response and the induction of cell death in plants. *Cell Death and Differentiation* **4**(8): 671-683.

Mou Z, Fan W, Dong X. 2003. Inducers of plant systemic acquired resistance regulate NPR1 function through redox changes. *Cell* **113**(7): 935-944.

Narusaka M, Shirasu K, Noutoshi Y, Kubo Y, Shiraishi T, Iwabuchi M, Narusaka Y. 2009. RRS1 and RPS4 provide a dual Resistance-gene system against fungal and bacterial pathogens. *Plant Journal* **60**(2): 218-226.

Pajerowska-Mukhtar KM, Emerine DK, Mukhtar MS. 2013. Tell me more: roles of NPRs in plant immunity. *Trends Plant Science* **18**(7): 402-411.

Periyannan S, Moore J, Ayliffe M, Bansal U, Wang X, Huang L, Deal K, Luo M, Kong X, Bariana H. 2013. The gene *Sr33*, an ortholog of barley *Mla* genes, encodes resistance to wheat stem rust race Ug99. *Science* **341**(6147): 786-788.

Pujol V, Robles J, Wang P, Taylor J, Zhang P, Huamh L, Table L, Lagudah E. 2016. Cellular and molecular characterization of a stem rust resistance locus on wheat chromosome 7AL. *BMC Research Notes* **9:**502.

Rate DN, Greenberg JT. 2001. The *Arabidopsis* aberrant growth and death2 mutant shows resistance to *Pseudomonas syringae* and reveals a role for NPR1 in suppressing hypersensitive cell death. *Plant Journal* **27**(3): 203-211.

Saini R, Kaur M, Singh B. Sharma S, Nanda GS. 2002. Genes *Lr48* and *Lr49* for hypersensitive adult plant leaf rust resistance in wheat (*Triticum aestivum* L.).

Euphytica **124:** 365–370.

Saucet SB, Ma Y, Sarris PF, Furzer OJ, Sohn KH, Jones JD. 2015. Two linked pairs of *Arabidopsis TNL* resistance genes independently confer recognition of bacterial effector AvrRps4. *Nature Communications* **6:** 6338.

Shirano Y, Kachroo P, Shah J, Klessig DF. 2002. A gain-of-function mutation in an *Arabidopsis* Toll interleukin1 receptor–nucleotide binding site–leucine-rich repeat type *R* gene triggers defense responses and results in enhanced disease resistance. *Plant Cell* **14**(12): 3149-3162.

Silverman P, Seskar M, Kanter D, Schweizer P, Metraux J-P, Raskin I. 1995. Salicylic acid in rice (biosynthesis, conjugation, and possible role). *Plant Physiology* **108**(2): 633-639.

Solovyev V, Kosarev P, Seledsov I, Vorobyev D. 2006. Automatic annotation of eukaryotic genes, pseudogenes and promoters. *Genome Biology* **7**, Suppl 1: P. 10.1-10.12.

Spoel SH, Dong X. 2012. How do plants achieve immunity? Defence without specialized immune cells. *Journal of Nature Reviews Immunology* **12**(2): 89.

Spoel SH, Koornneef A, Claessens SM, Korzelius JP, Van Pelt JA, Mueller MJ, Buchala AJ, Métraux J-P, Brown R, Kazan K. 2003. NPR1 modulates cross-talk between salicylate-and jasmonate-dependent defense pathways through a novel function in the cytosol. *Plant Cell* **15**(3): 760-770.

Spoel SH, Mou Z, Tada Y, Spivey NW, Genschik P, Dong X. 2009. Proteasome-mediated turnover of the transcription coactivator NPR1 plays dual roles in regulating plant immunity. *Cell* **137**(5): 860-872.

Stakman EC, Stewart DM, Loegering WQ. 1962. Identification of physiologic races of *Puccinia graminis* var. *tritici*. *U.S. Department of Agriculture, ARS* **E617:**5-53.

Wang X, Yang B, Li K, Kang Z, Cantu D, Dubcovsky J. 2016. A conserved *Puccinia striiformis* protein interacts with wheat NPR1 and reduces induction of pathogenesis-related genes in response to pathogens. *Molecular Plant-Microbe Interactions* **29**(12): 977-989.

Wang X, Wang Y, Liu P, Mu X, Liu X, Wang X, Zhao M, Huai B, Huang L, Kang Z. 2017.

TaRar1 is inovolved in wheat defense against stripe rust pathogen mediated by *YrSu*. *Frontiers in Plant Science* **8:**156.

Williams SJ, Sohn KH, Wan L, Bernoux M, Sarris PF, Segonzac C, Ve T, Ma Y, Saucet SB, Ericsson DJ. 2014. Structural basis for assembly and function of a heterodimeric plant immune receptor. *Science* **344:** 299–303.

Yuan Y, Zhong S, Li Q, Zhu Z, Lou Y, Wang L, Wang J, Wang M, Li Q, Yang D. 2007. Functional analysis of rice *NPR1*-like genes reveals that *OsNPR1/NH1* is the rice orthologue conferring disease resistance with enhanced herbivore susceptibility. *Plant biotechnology* **5**(2): 313-324.

Zhang X-C, Gassmann W. 2007. Alternative splicing and mRNA levels of the disease resistance gene *RPS4* are induced during defense responses. *Plant Physiology* **145**(4): 1577-1587.

Zhong X, Xi L, Lian Q, Luo X, Wu Z, Seng S, Yuan X, Yi M. 2015. The *NPR1* homolog *GhNPR1* plays an important role in the defense response of *Gladiolus hybridus*. *Plant cell reports* **34**(6): 1063-1074.

Zhang H, Qiu Y, Yuan C, Chen X, Huang L. 2018. Fine-tuning of *PR* genes in wheat responding to different Puccinia rust species. *Journal of Plant Physiology and Pathology.* **6:** 2

Figure captions

Figure 1: Wheat NPR1-like genes and organization & structures of the proteins. 1a: Genomic blot (Southern) hybridization result from genomic DNA of seven wheat NT lines and W3SNPR1 as a probe. Arrows indicate the chromosome location of each fragment. **1b:** Arrangement and structures of six *NPR1* homologs in wheat group 3 chromosomes. One dashed box represents one predicted gene and the arrow under each box indicates the orientation of the gene. The distance between the two *NPR1* homologs in the same chromosome is indicated in base-pair but not according to scale in the figure. Each colored box represents a region of a known functional domain. BTB: Broad complex, Tramtrack, and Bric-a`-brac; UK: DUF3420 Unknown domain;

Ank: Ankyrin repeats; NPR1_like_C: A region conserved at the NPR1 c-terminal; PKinase: Protein Kinase. The sizes of the domains are not according to scale. **1c:** Arrangement and structures of three *NPR1* homologs and three *NB-CC*-like genes in wheat chromosomes 7A, 7D and 4A(7B).

Figure 2: Infection types of *TaNPR1* knock-down assay. 2a: Infection types of *Sr33* near isogenic lines in Chinese Spring (CS) background when challenged with stem rust race QFCSC 14 days post inoculation. Leaves labeled with BSMV:G3, BSMV:4A+7D, BSMV:G3+G7; BSMV:G7 and BSMV:7A were from the plants that *TaNPR1* of groups 3, 4A+7D, group 3 & 7, only group 7 or only chromosome 7A were silenced, respectively. BSMV:00 plants were inoculated with BSMV without the target gene. BSMV:PDS plants were inoculated with BSMV plus PDS gene. CK plants that were not inoculated with BSMV are the mock control. **2b:** Infection types were quantified by a percentage of pustule area/leaf area. Each number is an average of three leaves. The same letter indicates the differences are not significant, and different letters indicate the differences are significant. * indicates the ρ value < 0.05. Each error bar shows the standard deviations among the three leaves.

Figure 3: Genomic DNA and two transcripts of the *Ta7ANPR1* gene. *Ta7ANPR1* has five exons. Under non-stressed growth conditions, the transcript retains the intron between exons 3 and 4, including a stop codon. The encoded peptide has 881 amino acids containing only the NB-ARC domain. Under stressed conditions, an additional transcript of *Ta7ANPR1* was detected. The alternative spliced isoform has the retained intron, and the stop codon removed, so the encoded peptide is 1,431 amino acids containing NB-ARC and NPR1.

Figure 4: Alternative splicing of the *Ta7ANPR1* locus. 4a: Reverse transcription amplified cDNAs from total RNAs extracted from CS under no-stressed condition, stripe rust inoculated or BSMV inoculated condition. An additional fragment was amplified from CS under stressed conditions. **4b:** Transcript of two isoforms of *Ta7ANPR1* in Cadenza during the time course of *Pgt* TPMKC infection. **4c:** Detection of two transcripts of *Ta7ANPR1* in the RNA-seq data generated

from *Lr47* near-isogenic lines post-*Pt* PBJJG inoculation at 6 time points. TPM: Transcripts Per Million. Each error bar shows the standard deviations among the three biological replicates.

Figure 5: Infection types of *Ta7ANPR1* mutants. 5a: Infection types of wild type Alpowa, mutant Al^{R805Q} and an F_1 of Alpowa/ Al^{R805Q} when challenged with stem rust race TPMKC 14 days post-inoculation. 5**b:** Infection types of wild type Cadenza and mutants of Cd^{A529E} and Cd^{M357I} at 14 days post-*Pgt* TPMKC inoculation. **5c:** Infection types of wild type Alpowa and mutant Al^{R805Q} at nine days post-*Pt* PBJJG inoculation. **5d:** Infection types of wild type Alpowa and mutant Al^{R805Q} at 17 days post-*Pst* CYR31 inoculation. **5e:** Infection types of wild type Alpowa and mutant Al^{R805Q} at 17 days post-*Pst* CYR23 inoculation. **5f:** Infection types were quantified by a percentage of pustule areas/leaf area. Each number is an average of three leaves. * indicates the ρ value < 0.05. ** indicates the ρ value < 0.01. Each error bar shows the standard deviations among the three leaves.

Figure 6: Models of *TaNPR1*-induced resistance and potential roles of TaNPR1 proteins during wheat-rust interactions. 6**a:** A model of resistance conferred by NPR1-dependent detection in an R protein complex by a pair of head-to-head NB-ARC genes. In wild-type during the absence of rusts, the two NB-ARC genes fold together in an inactive formation. In the presence of a rust pathogen, one of the NB-ARC loci produces an isoform protein containing NPR1 as a decoy. Two types of R protein complexes will be formed. If the rust secretes an effector to attack TaNPR1, the decoy NPR1 could be mistakenly attacked, and then the NPR1-decoy R protein complex will change to an active formation to induce defense response. Meanwhile, more NB-NPR1 isoform will be produced to distract the NPR1-attacking effector. In a mutant when a mutation resulted in a change of the R protein complex to an active formation, defense response is activated by the mutation. The mutant will be resistant to all rusts, except the

ones have effectors to suppress other components of the defense signaling pathway. **6b:** During wheat-rust interactions, rust pathogens may apply the invasion strategies including targeting TaG3NPR1 (Yes) or not (No). Without an ineffective detection system or compromised components for inducing defense signals, wheat will be susceptible to the pathogens. Resistant wheat to the "Yes" group of rusts may use TaNPR1 as a decoy (e.g., Ta7ANPR1) in the detection and have an alternative pathway bypass TaNPR1 once the integrity of the NPR1 is compromised by the pathogens. Resistant wheat to the "No" group of rusts may use either NPR1-independent (e.g., *Sr33*) or NPR1-dependent signaling through TaG3NPR1. Whether a defense signaling could be transduced by both NPR1-dependent/independent is a question mark.

Supporting Information

Notes S1: Amino acid sequences and the location of each predicted functional domain of the TaNPR1 proteins in Fig. 1b, c.

Notes S2: The alignment of the cDNAs of the *TaG3NPR1* genes and the location of the target region for silencing.

Notes S3: The alignment of the cDNAs of the *TaG7NPR1* genes and the location of the target region for silencing.

Figure S1: Specificity of primers for screening mutations on *Ta7ANPR1*.

Figure S2: Transcripts of *Ta7ANPR1, Ta4ANPR1* and *Ta7DNPR1* during the time course of rust infections.

Figure S3: SA/JA concentrations and *PR* gene expressions when the *TaG3NPR1* genes were down-regulated.

Figure S4: Transcripts of *TaG3NPR1* and *TaG3Kinase-NPR1* during the time course of *Pst* infection.

Figure S5: *PR* gene expressions when the *Ta7ANPR1* gene was down-regulated.

Figure S6: *PR* gene expressions in the wild types and mutants without pathogen inoculation.

Figure S7: *PR1* and *PR10* expressions during a time-course post-*Pgt* inoculation.

Table S1: Sequences of the Oligos used to construct silencing constructs.

Table S2: Sequences of the primers used for quantitative real-time PCR and mutant screening.

Table S3: Real-time qPCR analysis of *TaNPR1*-like gene expression levels in silenced plants.

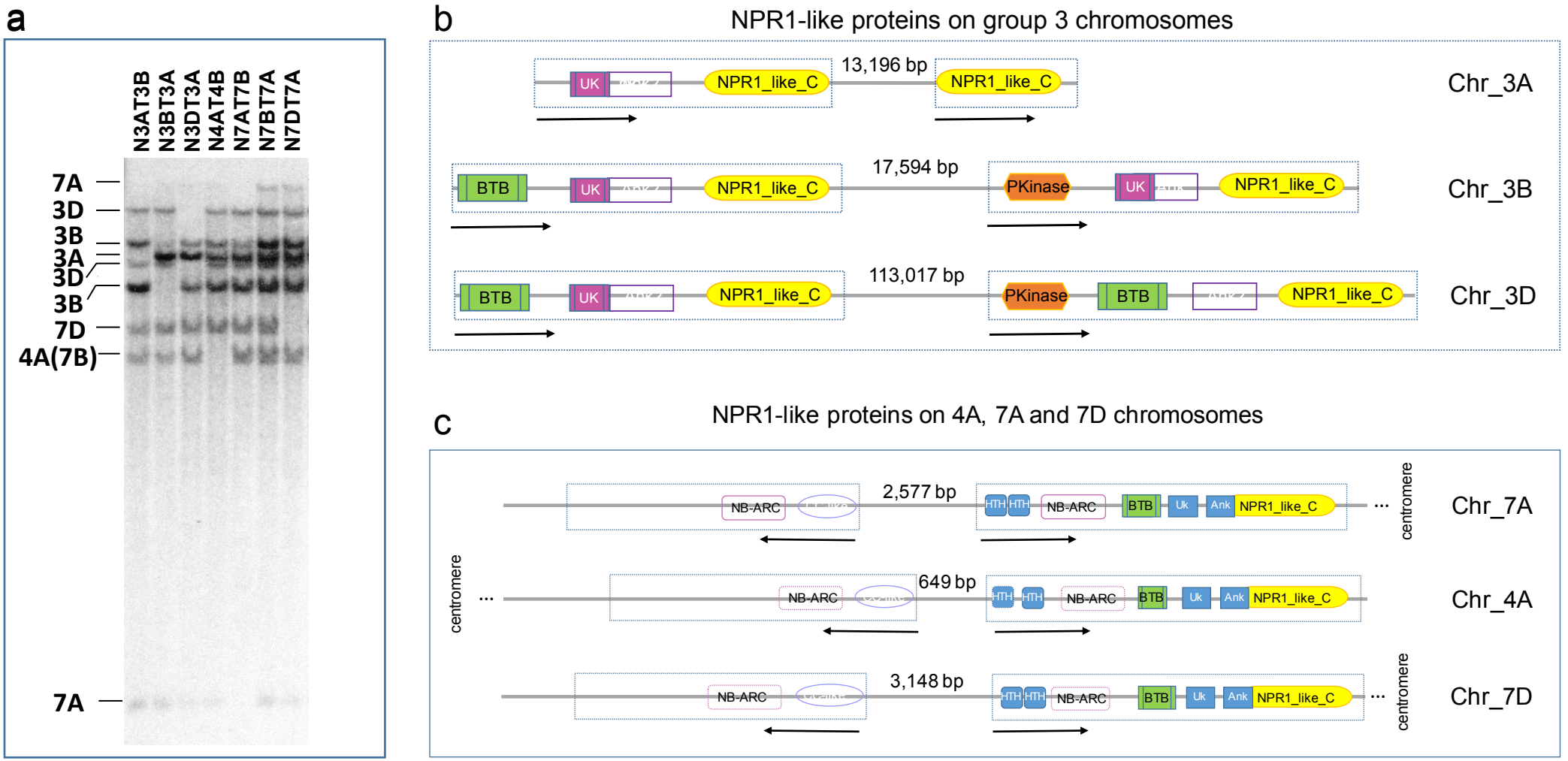
a
N3AT3B
N3BT3A
N3DT3A
N4AT4B
N7AT7B
N7BT7A
N7DT7A
7A
3D
3B
3A
3D
3B
7D
4A(7B)
7A
b
NPR1-like proteins on group 3 chromosomes
13,196 bp
UK
NPR1_like_C
NPR1_like_C
Chr_3A
17,594 bp
BTB
UK
NPR1_like_C
PKinase
UK
NPR1_like_C
Chr_3B
113,017 bp
BTB
UK
NPR1_like_C
PKinase
BTB
NPR1_like_C
Chr_3D
c
NPR1-like proteins on 4A, 7A and 7D chromosomes
2,577 bp
NB-ARC
HTH
HTH
NB-ARC
BTB
Uk
Ank
NPR1_like_C
centromere
Chr_7A
649 bp
centromere
NB-ARC
HTH
HTH
NB-ARC
BTB
Uk
Ank
NPR1_like_C
Chr_4A
3,148 bp
NB-ARC
HTH
HTH
NB-ARC
BTB
Uk
Ank
NPR1_like_C
centromere
Chr_7D

Figure 1

a

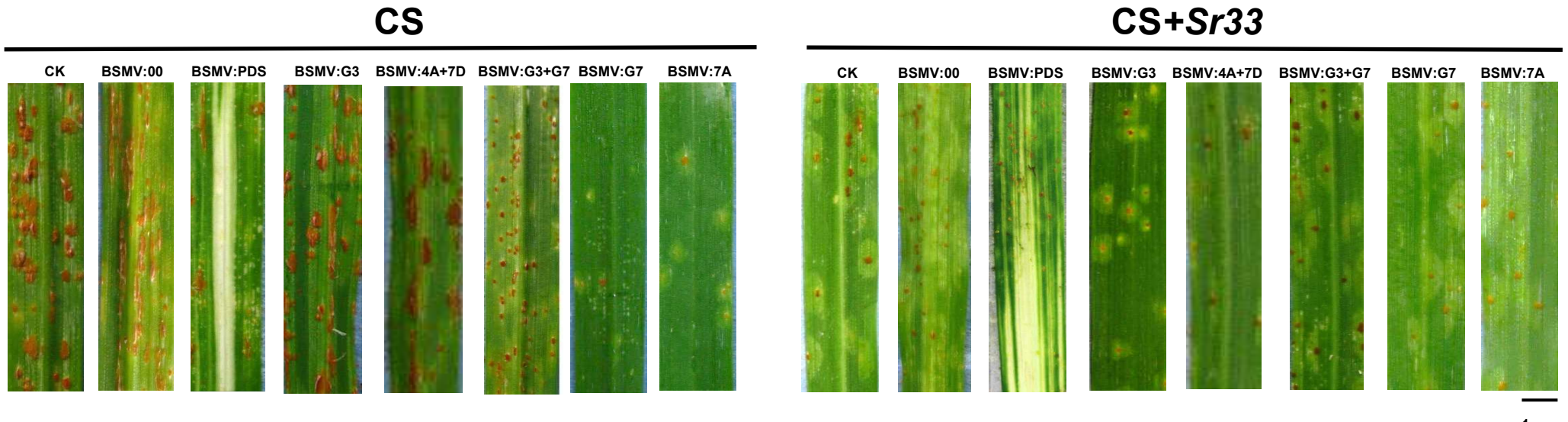
CS
CS+Sr33
CK
BSMV:00
BSMV:PDS
BSMV:G3
BSMV:4A+7D
BSMV:G3+G7
BSMV:G7
BSMV:7A
1cm

b

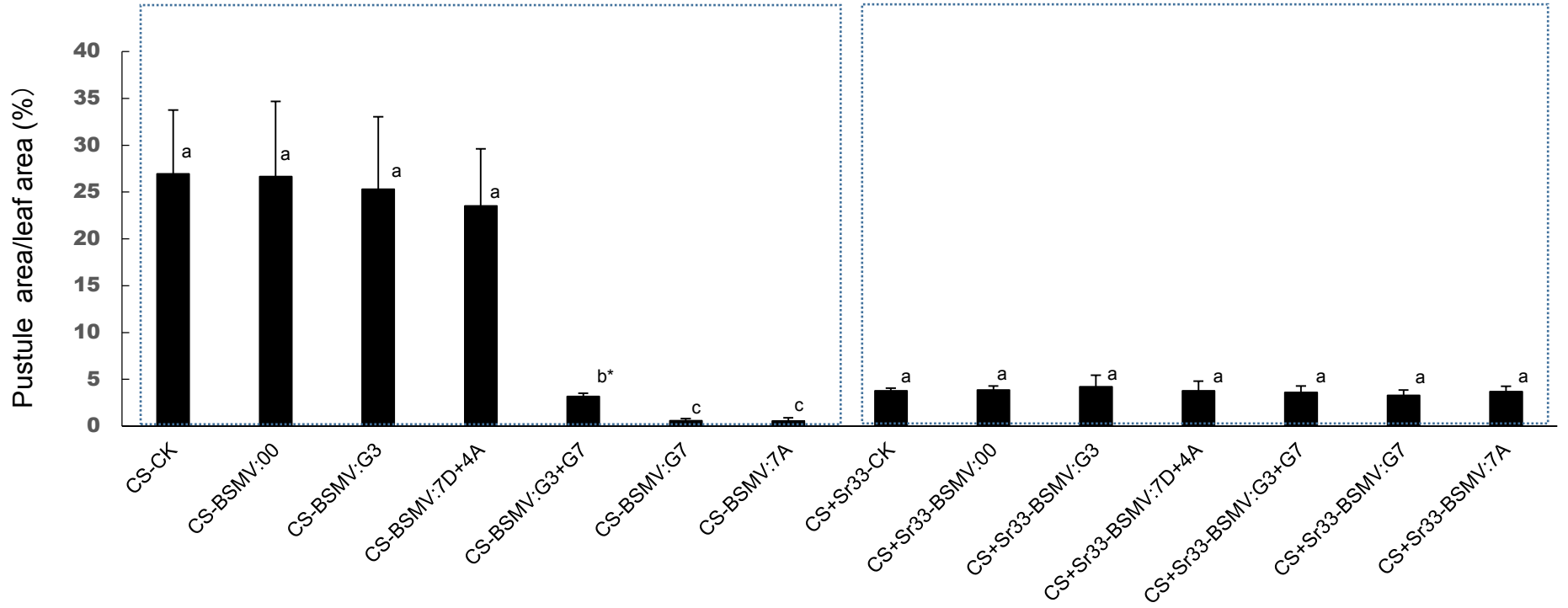
Pustule area/leaf area (%)
0
5
10
15
20
25
30
35
40
a
a
a
a
b*
c
c
a
a
a
a
a
a
a
CS-CK
CS-BSMV:00
CS-BSMV:G3
CS-BSMV:7D+4A
CS-BSMV:G3+G7
CS-BSMV:G7
CS-BSMV:7A
CS+Sr33-CK
CS+Sr33-BSMV:00
CS+Sr33-BSMV:G3
CS+Sr33-BSMV:7D+4A
CS+Sr33-BSMV:G3+G7
CS+Sr33-BSMV:G7
CS+Sr33-BSMV:7A

Figure 2

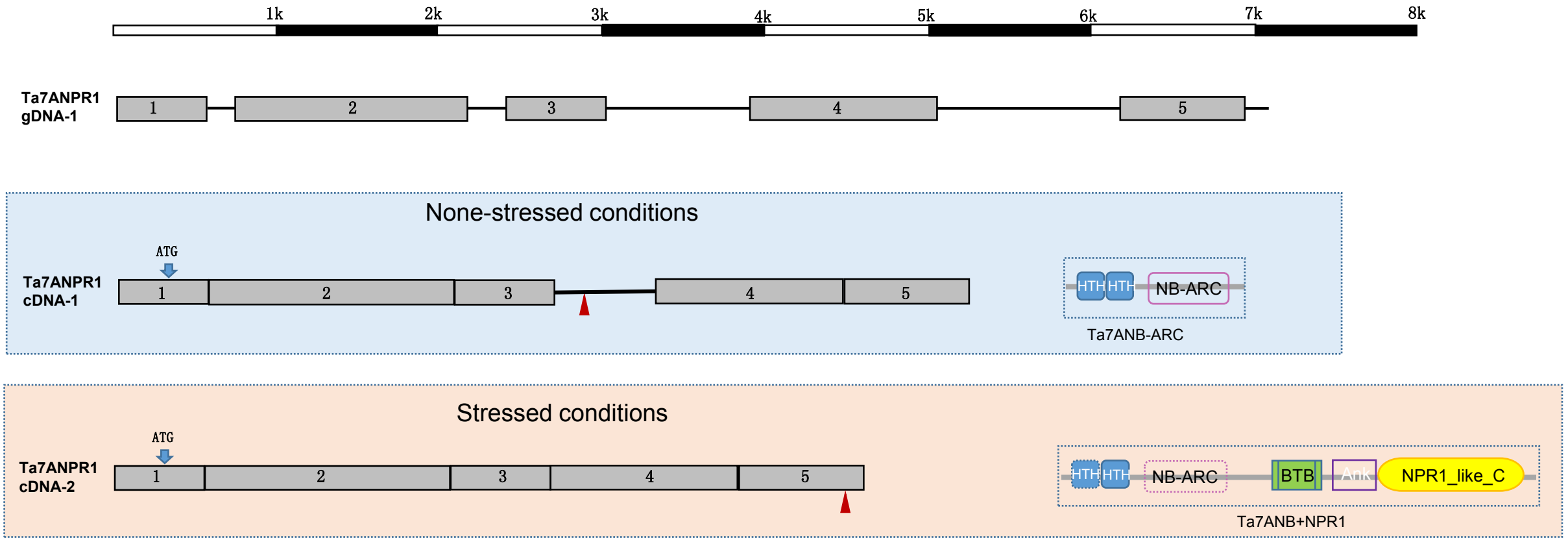
1k
2k
3k
4k
5k
6k
7k
8k
Ta7ANPR1
gDNA-1
1
2
3
4
5
None-stressed conditions
ATG
Ta7ANPR1
cDNA-1
1
2
3
4
5
HTH
HTH
NB-ARC
Ta7ANB-ARC
Stressed conditions
ATG
Ta7ANPR1
cDNA-2
1
2
3
4
5
HTH
HTH
NB-ARC
BTB
Ank
NPR1_like_C
Ta7ANB+NPR1

Figure 3

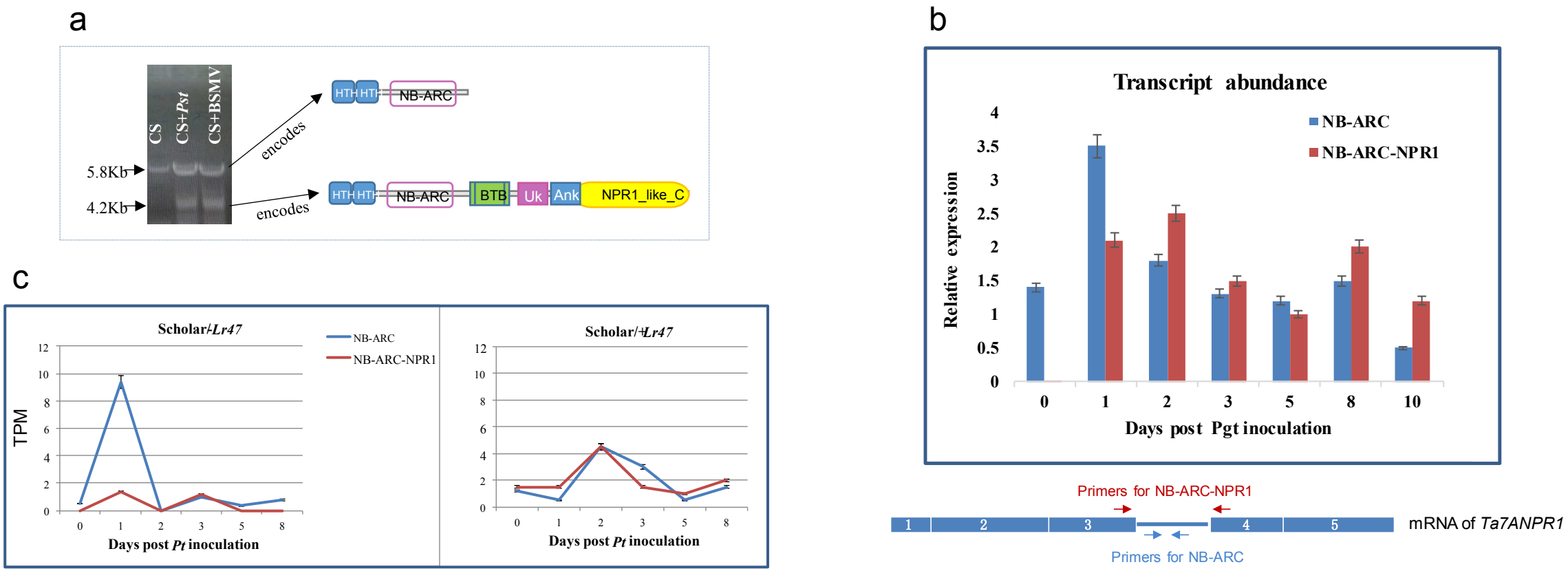
a
CS
CS+Pst
CS+BSMV
5.8Kb
4.2Kb
encodes
encodes
HTH HTH
NB-ARC
HTH HTH
NB-ARC
BTB
Uk
Ank
NPR1_like_C
b
Transcript abundance
NB-ARC
NB-ARC-NPR1
Relative expression
Days post Pgt inoculation
Primers for NB-ARC-NPR1
Primers for NB-ARC
mRNA of Ta7ANPR1
c
Scholar/-Lr47
Scholar/+Lr47
NB-ARC
NB-ARC-NPR1
TPM
Days post Pt inoculation

Figure 4

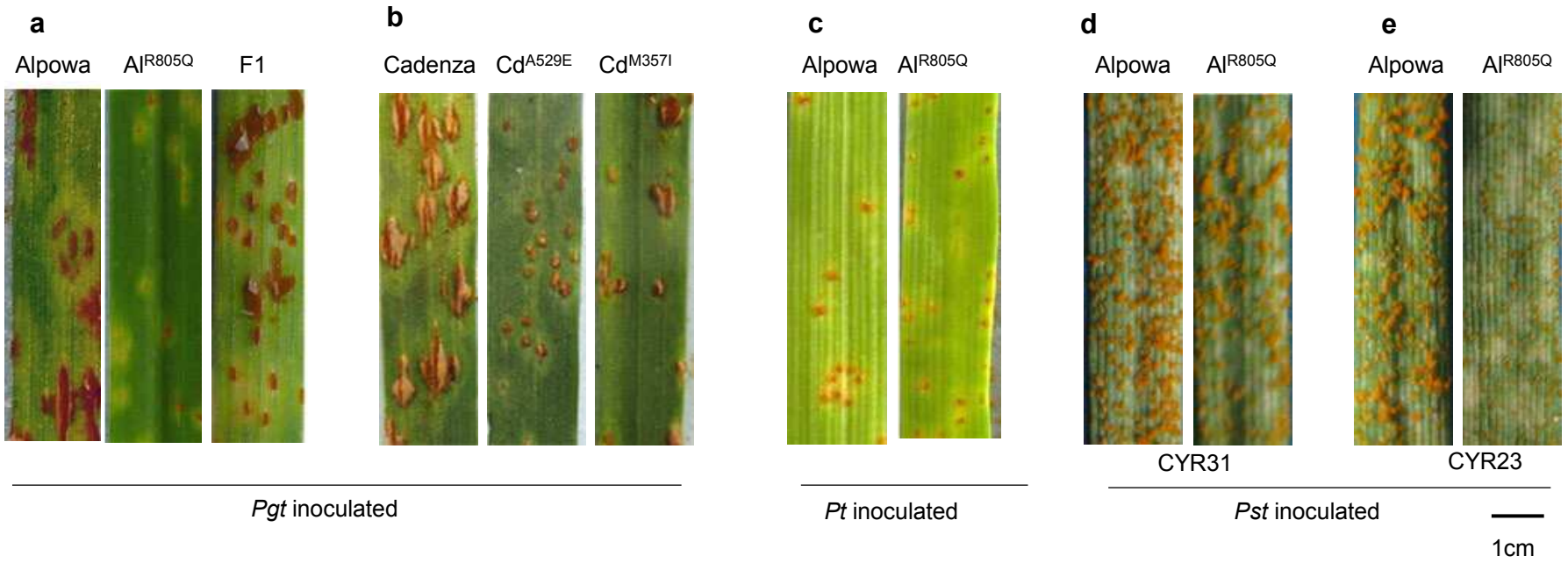
a
Alpowa
AlR805Q
F1
b
Cadenza
CdA529E
CdM357I
c
Alpowa
AlR805Q
d
Alpowa
AlR805Q
CYR31
e
Alpowa
AlR805Q
CYR23
Pgt inoculated
Pt inoculated
Pst inoculated
1cm

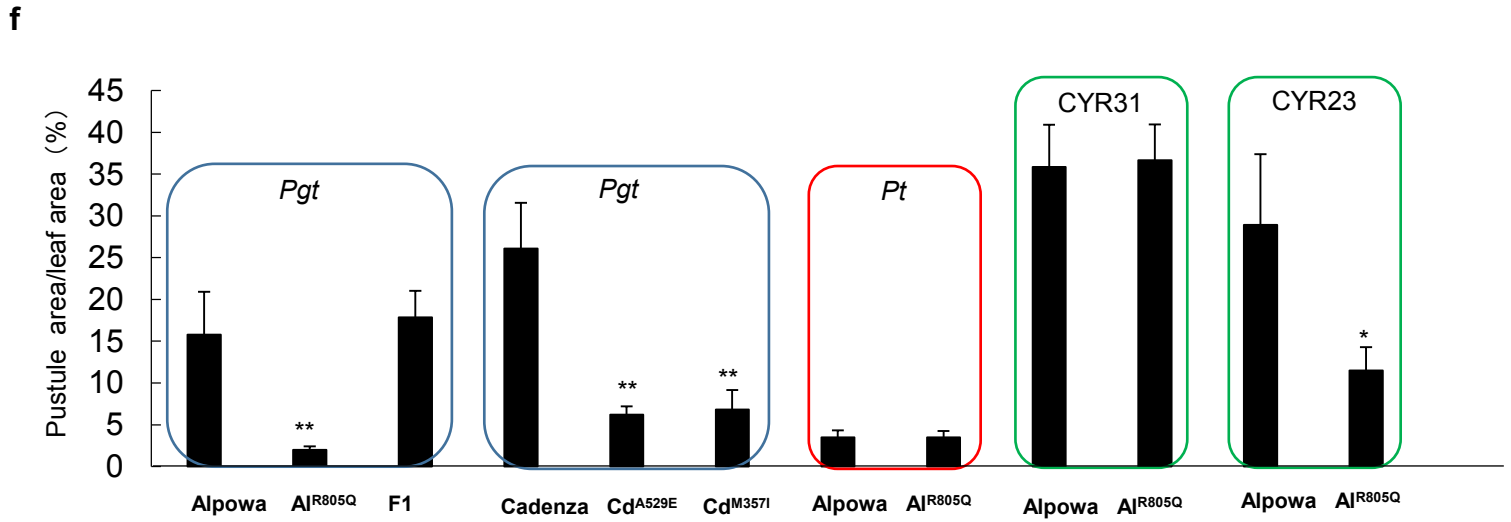
f
Pustule area/leaf area (%)
45
40
35
30
25
20
15
10
5
0
Pgt
Pgt
Pt
CYR31
CYR23
**
**
**
*
Alpowa
AlR805Q
F1
Cadenza
CdA529E
CdM357I
Alpowa
AlR805Q
Alpowa
AlR805Q
Alpowa
AlR805Q

Figure 5

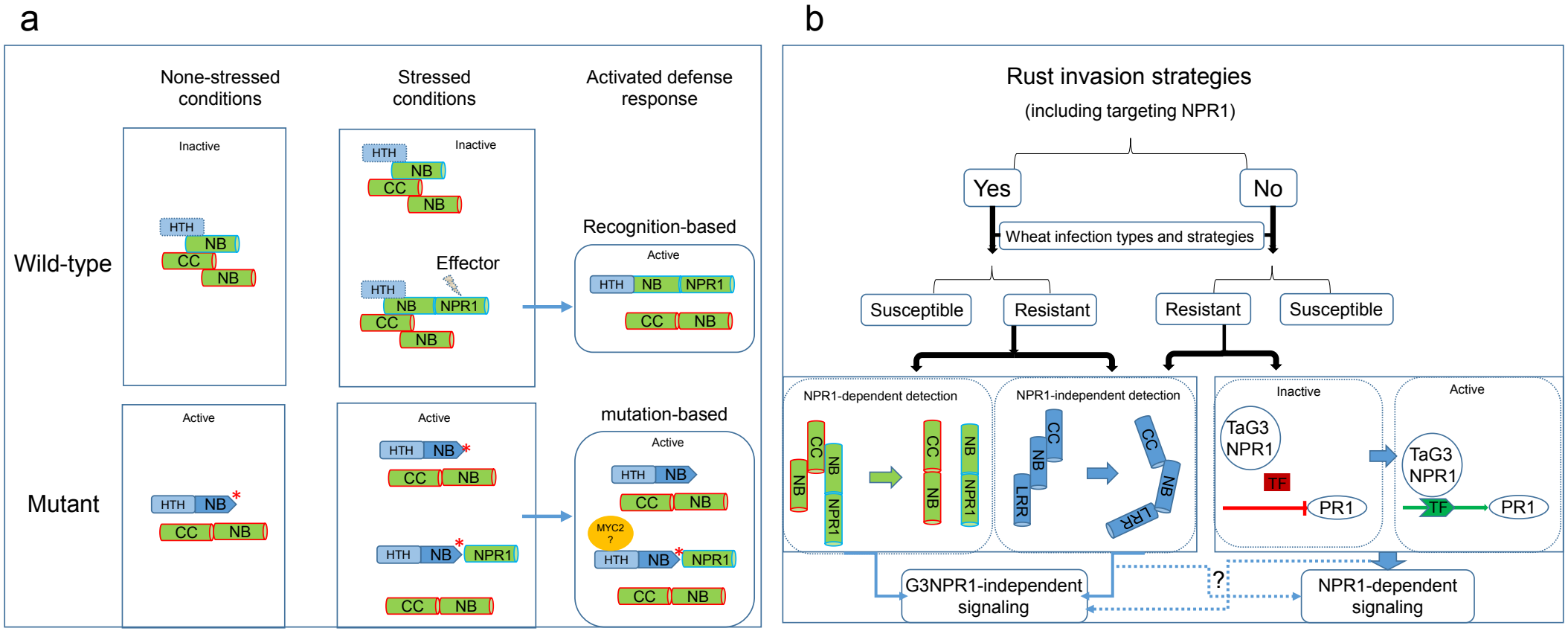
a
None-stressed conditions
Stressed conditions
Activated defense response
Wild-type
Mutant
Inactive
Active
HTH
NB
CC
NB
Effector
NPR1
Recognition-based
mutation-based
MYC2 ?
b
Rust invasion strategies
(including targeting NPR1)
Yes
No
Wheat infection types and strategies
Susceptible
Resistant
Resistant
Susceptible
NPR1-dependent detection
NPR1-independent detection
LRR
TaG3 NPR1
TF
PR1
G3NPR1-independent signaling
?
NPR1-dependent signaling

Figure 6